Density Functional Theory for Block Copolymer Melts and Blends

2 AUTHORS, INCLUDING:

Masao Doi

137 PUBLICATIONS 2,422 CITATIONS

SEE PROFILE

Density Functional Theory for Block Copolymer Melts and Blends

Takashi Uneyama[1] and Masao Doi[2]

[1] Department of Computational Science and Engineering,
Graduate School of Engineering, Nagoya University,
Chikusa, Nagoya, JAPAN
[2] Department of Applied Physics,
Graduate School of Engineering, The University of Tokyo,
Hongo, Tokyo, JAPAN

Abstract

We derive an expression for the free energy of the blends of block copolymers expressed as a functional of the density distribution of the monomer of each block. The expression is a generalization of the Flory-Huggins-de Gennes theory for homo polymer blends, and also a generalization of the Ohta-Kawasaki theory for the melts of diblock copolymers. The expression can be used for any blends of homopolymers and block copolymers of any topological structure. The expression gives a fast and stable computational method to calculate the micro and macro phase separation of the blends of homopolymers and block copolymers.

1 Introduction

Block copolymers and their blends show various interesting micro structures in equilibrium due to the difference in the segmental interaction between the polymer blocks [1]. The phenomena has been extensively studied by the self consistent field (SCF) theory [2, 3, 4, 5, 6, 7, 8, 9, 10, 11] in which the free energy of the system is calculated by evaluating the path integral (or by solving the Edwards equation) for each polymers in the mean field. This method is quite useful as it can calculate the free energy of any blends of polymers of arbitrary topological structure. On the other hand, the SCF calculation is computationally demanding as it needs large memory and large CPU power.

Many works have been done to reduce the CPU time and the memory needed for the SCF calculation. If the system has a periodic structure of known symmetry, the equilibrium structure (or the local equilibrium structure for the given symmetry) can be calculated rather efficiently by obtaining the eigen functions for the Edwards equation [3, 4], or by using the narrow interface approximation and the unit cell approximation [2, 4]. On the other hand,if the system does not have periodic structure (such as in the case of micellar systems) or if the symmetry of the system is not known, other strategies are needed to get equilibrium structures. Fraaije and his coworkers developed a theory for the dynamics and conducted several dynamic simulations, such as the dynamic behavior of the block copolymer melts under shear flow or the aqueous solution of the block copolymers [5, 6, 7]. Fredrickson et. al. proposed an efficient SCF algorithm for real space simulation [8], and introduced complex fields to improve the efficiency of convergence [9].

Though significant progress has been made in the SCF calculation, it is still very difficult to simulate the 3 dimensional large systems of reasonable size of polymers as the required computational resources increase dramatically with the increase of the chain length: for 3 dimensional simulation, the calculation is practically limited to the system where the effective degree of polymerization is not so large.

An alternative approach is the density functional (DF) theory first introduced by Leibler [12]. In this approach, the free energy F of the system is expressed as a functional of the density distribution function of each monomer species. Clearly the computational cost of such approach is much less than that of the SCF calculation since the evaluation of the path integral which costs the major part of the cpu time and memory in the SCF calculation is not needed. For example, consider to simulate the block copolymer solutions: the degrees of polymerization of solvents are unity and ones of block copolymers are large. We cannot assume any periodicity for such a systems, thus we need to do the real space simulation. The computational cost of the SCF calculation increases dramatically as the degrees of polymerization of block copolymers increase, while the cost of the DF simulations is independent of the degree of polymerization.

In the first DF theory [12] applied to AB type diblock copolymers, the density functional was obtained as a power series of $\delta\phi(\boldsymbol{r}) = \phi(\boldsymbol{r}) - \bar{\phi}$, where $\phi(\boldsymbol{r})$ is the volume fraction of A segment at point $\boldsymbol{r}$, and $\bar{\phi}$ is the spatial average of $\phi(\boldsymbol{r})$.

$$\bar{\phi} = \frac{1}{V} \int d\boldsymbol{r}\phi(\boldsymbol{r}) \tag{1}$$

where V is the volume of the system. The free energy is expressed as [10]

$$
\begin{aligned}
F\left[\phi(\boldsymbol{r})\right] = &\, F\left[\bar{\phi}\right] \\
&+ \frac{1}{2} \int d\boldsymbol{r}d\boldsymbol{r}'\, \Gamma(\boldsymbol{r} - \boldsymbol{r}')\delta\phi(\boldsymbol{r})\delta\phi(\boldsymbol{r}') \\
&+ \frac{1}{3!} \int d\boldsymbol{r}d\boldsymbol{r}'d\boldsymbol{r}''\, \Gamma^{(3)}(\boldsymbol{r} - \boldsymbol{r}', \boldsymbol{r} - \boldsymbol{r}'')\delta\phi(\boldsymbol{r})\delta\phi(\boldsymbol{r}')\delta\phi(\boldsymbol{r}'') \\
&+ \cdots
\end{aligned}
\tag{2}
$$

where $F\left[\bar{\phi}\right]$ is the free energy for homogeneous state. The vertex functions $\Gamma(\boldsymbol{r})$, and $\Gamma^{(3)}(\boldsymbol{r}, \boldsymbol{r}')$ are calculated by solving the Edwards equation or by calculating the density correlation functions.

Leibler's method is mathematically sound, but it can be applied only for the the case of weak segregation, i.e., the case that the deviation from the homogeneous state is small. In order to apply the DF theory to the strong segregation case, Ohta and Kawasaki proposed an approximate expression for the free energy [13, 14]. They noticed that in Leibler's theory, the term which is essential for giving the micro phase separation is the "long range" term. This term appears in the limit of small wave vector $\boldsymbol{q}$ in the Fourier transform of $\Gamma(\boldsymbol{r})$

$$\Gamma(\boldsymbol{q}) = \int d\boldsymbol{r}e^{-i\boldsymbol{q}\cdot\boldsymbol{r}}\Gamma(\boldsymbol{r}) \tag{3}$$

For small wave vector $\boldsymbol{q}$, $\Gamma(\boldsymbol{q})$ diverges as follows:

$$\Gamma(\boldsymbol{q}) = \frac{A}{\boldsymbol{q}^2} \qquad \text{for} \quad \boldsymbol{q}^2 \to 0 \tag{4}$$

where A is a certain constant. The divergence comes from the fact that the monomer A of block copolymers are always connected to monomer B and therefore cannot separate from monomer B further than the size of the block polymer. Ohta and Kawasaki then proposed the following form of the free energy functional for the diblock polymer:

$$F\left[\phi(\boldsymbol{r})\right] = F_L\left[\phi(\boldsymbol{r})\right] + F_S\left[\phi(\boldsymbol{r})\right] \tag{5}$$

where $F_L\left[\phi(\boldsymbol{r})\right]$ and $F_S\left[\phi(\boldsymbol{r})\right]$ stands for the free energy due to the long range and short range interactions. The long range part is expressed as

$$F_L\left[\phi(\boldsymbol{r})\right] = \int d\boldsymbol{r}d\boldsymbol{r}'\, \frac{A}{2}\mathcal{G}(\boldsymbol{r} - \boldsymbol{r}')\delta\phi(\boldsymbol{r})\delta\phi(\boldsymbol{r}') \tag{6}$$

where $\mathcal{G}(\boldsymbol{r})$ is the inverse Fourier transform of $1/\boldsymbol{q}^2$.

$$\mathcal{G}(\boldsymbol{r}) = \frac{1}{(2\pi)^d} \int d\boldsymbol{q}e^{i\boldsymbol{q}\cdot\boldsymbol{r}}\frac{1}{\boldsymbol{q}^2} \tag{7}$$

where d is the dimension of the space. In the real space, $\mathcal{G}(\boldsymbol{r} - \boldsymbol{r}')$ satisfies

$$-\nabla^2 \mathcal{G}(\boldsymbol{r} - \boldsymbol{r}') = \delta(\boldsymbol{r} - \boldsymbol{r}') \tag{8}$$

As to the short range part, Ohta and Kawasaki assumed the Cahn-Hilliard free energy:

$$F_S\left[\phi(\boldsymbol{r})\right] = \int d\boldsymbol{r} \left[\frac{B}{2}\left|\nabla\phi(\boldsymbol{r})\right|^2 + f\left(\phi(\boldsymbol{r})\right)\right] \tag{9}$$

where B is a constant and $f\left(\phi(\boldsymbol{r})\right)$ is a certain function which has double minima.

As the Ohta-Kawasaki theory involves a few intuitive arguments, generalization of the theory to other systems was not straightforward. Indeed the generalization has been done only for limited systems such as the ABC triblock copolymers [15, 16], the blends of AB diblock copolymer and C homopolymer [17], and the blends of A homopolymer, B homopolymer and AB diblock copolymer [18].

In this paper we propose a general expression for the free energy which can be applied for any types of block copolymers and their blends. All parameters in the free energy are expressed by the microscopic parameters appearing in the SCF theory, i.e., the structure of block copolymers and the interaction parameters (the χ parameters). This expression gives a fast computational method to calculate the equilibrium structure formed by the blends of block polymers.

An approach similar to ours was already taken by Bohbot-Raviv and Wang [19]: they proposed an approximate expression for the free energy functional which can be applied for arbitrary structure of block polymers. We will compare our theory with their theories later.

The present paper is constructed as follows. Firstly, we obtain the free energy functional for the situation that the deviation from the homogeneous state is small. This step is rather straightforward: the free energy is obtained by using the standard procedure of the linearized mean field approximation, often referred to as the random phase approximation (RPA) [20, 10]. Secondly we generalize this expression and seek an expression which can be applied for the situation that the density deviation from the homogeneous state is large. The second step is rather arbitrary, but we found an expression which reduces to the Flory-Huggins-de Gennes theory for homopolymer blends [21] and to Ohta-Kawasaki theory for the melts of diblock copolymers. Thirdly we test this expression of the free energy by comparing the results of this expression with that of the SCF theory, and discuss the validity of the expression.

2 Free Energy Functional for Small Density Perturbation

2.1 The Second Order Vertex Function

We consider a mixture of homo polymers and block copolymers which consist of several types of monomer units A, B, C.... The chemical structure of block copolymers are characterized by the species of monomer units (such as A,B,C...), the number of monomers in each block, and the connectivity of these blocks. Polymers having the same chemical structure, i.e., polymers consisting of the same blocks (of same monomer units and of same length) connected in the same way are regarded to belong to the same polymer type. The polymer type is distinguished by the suffices $p, q, r, \dots$, and each block in the polymer is distinguished by the suffices, $i, j, k, \dots$ (see Figure 1).

Let N_{pi} be the number of monomers belonging to the the i-th block of polymer p. The total number of monomers in the polymer p is given by

$$N_p = \sum_i N_{pi} \tag{10}$$

The block-ratio of the i-th block of polymer p is defined by

$$f_{pi} \equiv \frac{N_{pi}}{N_p} \tag{11}$$

We assume that all monomer units A,B,.. have the same specific volume and same bond length (this assumption can be removed but here it is assumed for the sake of simplicity). Let $\phi_{pi}(\boldsymbol{r})$ be the volume fraction of the monomer belonging to the block (p,i) at point $\boldsymbol{r}$. Our objective is to find out the free energy expressed as a functional of $\{\phi_{pi}(\boldsymbol{r})\}$.

We first consider the situation that the system is homogeneous at equilibrium, and calculate the change of the free energy for small density variation. In the homogeneous state, $\phi_{pi}(\boldsymbol{r})$ is equal to

$$\bar{\phi}_{pi} = f_{pi}\bar{\phi}_p. \tag{12}$$

Let $\delta\phi_{pi}(\boldsymbol{r}) = \phi_{pi}(\boldsymbol{r}) - f_{pi}\bar{\phi}_p$ be the deviation of the monomer distribution from the homogeneous state. The free energy functional for the system can be expressed as a quadratic form of $\delta\phi_{pi}(\boldsymbol{r})$ [12, 13].

$$
\begin{aligned}
F\left[\{\phi_{pi}(\boldsymbol{r})\}\right] = {}& F\left[\{f_{pi}\bar{\phi}_p\}\right] \\
& + \frac{1}{2}\sum_{pi,qj}\int d\boldsymbol{r}d\boldsymbol{r}'\,\Gamma_{pi,qj}(\boldsymbol{r}-\boldsymbol{r}')\delta\phi_{pi}(\boldsymbol{r})\delta\phi_{qj}(\boldsymbol{r}') \\
& + \cdots
\end{aligned}
\tag{13}
$$

where $F\left[\{f_{pi}\bar{\phi}_p\}\right]$ is the free energy for the homogeneous state, and $\Gamma_{pi,qj}(\boldsymbol{r}-\boldsymbol{r}')$ is the second order vertex function. In the Fourier space, eq (13) can be written as follows

$$
\begin{aligned}
F\left[\{\phi_{pi}(\boldsymbol{q})\}\right] = {}& F\left[\{f_{pi}\bar{\phi}_p\}\right] \\
& + \frac{1}{2}\sum_{pi,qj}\frac{1}{(2\pi)^d}\int d\boldsymbol{q}\,\Gamma_{pi,qj}(\boldsymbol{q})\delta\phi_{pi}(-\boldsymbol{q})\delta\phi_{qj}(\boldsymbol{q}) \\
& + \cdots
\end{aligned}
\tag{14}
$$

where $\delta\phi_{pi}(\boldsymbol{q})$ and $\Gamma_{pi,qj}(\boldsymbol{q})$ are the Fourier transform of $\delta\phi_{pi}(\boldsymbol{r})$ and $\Gamma_{pi,qj}(\boldsymbol{r})$:

$$\delta\phi_{pi}(\boldsymbol{q}) = \int d\boldsymbol{r}\,e^{-i\boldsymbol{q}\cdot\boldsymbol{r}}\delta\phi_{pi}(\boldsymbol{r}) \tag{15}$$

$$\Gamma_{pi,qj}(\boldsymbol{q}) = \int d\boldsymbol{r}\,e^{-i\boldsymbol{q}\cdot\boldsymbol{r}}\Gamma_{pi,qj}(\boldsymbol{r}) \tag{16}$$

The second order vertex function $\Gamma_{pi,qj}(\boldsymbol{q})$ determines the density fluctuation in the homogeneous state and can be related to the density correlation function $S_{pi,qj}(\boldsymbol{q})$ which is defined by

$$S_{pi,qj}(\boldsymbol{q}) = \langle\delta\phi_{pi}(\boldsymbol{q})\delta\phi_{qj}(-\boldsymbol{q})\rangle \tag{17}$$

where $\langle\ldots\rangle$ stands for the ensemble average for the equilibrium state. The density correlation function $S_{pi,qj}(\boldsymbol{q})$ is related to $\Gamma_{pi,qj}(\boldsymbol{q})$ by the following equation:

$$\sum_{q,j}\Gamma_{pi,qj}(\boldsymbol{q})S_{qj,rk}(\boldsymbol{q}) = \delta_{pr}\delta_{ik} \tag{18}$$

For ideal chains for which there is no interaction between monomer units, the density correlation arises from the connectivity of the polymer chain, and exists only for the monomers belonging to the same polymer chain. Hence $S_{pi,qj}(\boldsymbol{q})$ for the ideal chain is written as:

$$S_{pi,qj}^{(\text{ideal})}(\boldsymbol{q}) = \bar{\phi}_p\delta_{pq}h_{p,ij}(\boldsymbol{q}) \tag{19}$$

where $h_{p,ij}(\boldsymbol{q})$ is the correlation function for a single chain. Let $\boldsymbol{r}_{pi}^{(s)}$ be the position of the s-th monomer in the i-th block of the polymer p, then $h_{p,ij}(\boldsymbol{q})$ is given by

$$h_{p,ij}(\boldsymbol{q}) = \frac{1}{N_p}\int_0^{N_{pi}}ds\int_0^{N_{pj}}ds'\left\langle\exp\left[i\boldsymbol{q}\cdot(\boldsymbol{r}_{pi}^{(s)}-\boldsymbol{r}_{pj}^{(s')})\right]\right\rangle \tag{20}$$

4

For Gaussian chain, the average can be calculated easily to give

$$
h_{p,ij}(\boldsymbol{q}) =
\begin{cases}
\dfrac{2N_p f_{pi}^2}{\xi_{pi}^2}\left(e^{-\xi_{pi}} - 1 + \xi_{pi}\right) & (i = j) \\[4mm]
\dfrac{N_p f_{pi} f_{pj}}{\xi_{pi}\xi_{pj}}\left(e^{-\xi_{pi}} - 1\right)\left(e^{-\xi_{pj}} - 1\right)e^{-l_{p,ij}^2 \boldsymbol{q}^2/6} & (i \neq j)
\end{cases}
\tag{21}
$$

where

$$
\xi_{pi} = \frac{1}{6}N_p f_{pi} b^2 \boldsymbol{q}^2
\tag{22}
$$

b is the effective bond length and

$$
l_{p,ij}^2 = M_{p,ij} b^2
\tag{23}
$$

Here $M_{p,ij}$ is the number of monomers included in the shortest path connecting the i-th block and the j-th block of the p-th polymer, i.e., the chemical distance between the i-j blocks.

Thus for ideal chains, the correlation function can be calculated by eqs (19) and (21), and the vertex function can be calculated by eq (18). This gives the following expression for the vertex function of the ideal chain $\Gamma_{pi,qj}^{(\text{ideal})}(\boldsymbol{q})$:

$$
\Gamma_{pi,qj}^{(\text{ideal})}(\boldsymbol{q}) = \frac{\delta_{pq}}{\phi_p}g_{p,ij}(\boldsymbol{q})
\tag{24}
$$

where $g_{p,ij}(\boldsymbol{q})$ is the inverse of the matrix $h_{p,ij}(\boldsymbol{q})$:

$$
\sum_j h_{p,ij}(\boldsymbol{q})g_{p,jk}(\boldsymbol{q}) = \delta_{ik}
\tag{25}
$$

The effect of the interaction among the monomer units can be taken into account by adding the following interaction energy term

$$
F_{\text{int}}\left[\{\phi_{pi}(\boldsymbol{r})\}\right] = \frac{1}{2}\sum_{pi,qj}\int d\boldsymbol{r}\,\chi_{pi,qj}\phi_{pi}(\boldsymbol{r})\phi_{qj}(\boldsymbol{r})
\tag{26}
$$

where $\chi_{pi,qj}$ is the χ parameter for the interaction between the monomers in the block (p,i) and those in the block (q,j). Eqs (24) and (26) give the following vertex function:

$$
\Gamma_{pi,qj}(\boldsymbol{q}) = \frac{\delta_{pq}}{\phi_p}g_{p,ij}(\boldsymbol{q}) + \chi_{pi,qj}
\tag{27}
$$

2.2 Asymptotic Behavior of the Vertex Function for Large and Small Wave Vector

Though $\Gamma_{pi,qj}(\boldsymbol{q})$ can be obtained by the formula given above, it is desirable to have an analytical expression for $\Gamma_{pi,qj}(\boldsymbol{q})$. As it was first noticed by Leibler [12], the characteristics of $\Gamma_{pi,qj}(\boldsymbol{q})$ is that it diverges as $1/\boldsymbol{q}^2$ for small $\boldsymbol{q}$. Ohta and Kawasaki utilized this fact in deriving their approximate density functional for the free energy of diblock copolymers. The divergence of $\Gamma_{pi,qj}(\boldsymbol{q})$ for small $\boldsymbol{q}$ reflects the topological structure of the block copolymer. The vertex function $\Gamma_{pi,qj}(\boldsymbol{q})$ also diverges for large $\boldsymbol{q}$ region in such a way as $\Gamma_{pi,qj}(\boldsymbol{q}) \propto \boldsymbol{q}^2$. Our strategy of constructing the approximate free energy functional is to get an expression which correctly describe the asymptotic behavior of $\Gamma_{pi,qj}(\boldsymbol{q})$ for large $\boldsymbol{q}$ and small $\boldsymbol{q}$ region. Therefore we first study the behavior of $g_{p,ij}(\boldsymbol{q})$ for large $\boldsymbol{q}$ and small $\boldsymbol{q}$ region.

For large $\boldsymbol{q}$, the behavior of $g_{p,ij}(\boldsymbol{q})$ is easily seen. In the limit of $\boldsymbol{q}^2 \to \infty$, the correlation function $h_{p,ij}(\boldsymbol{q})$ is totally determined by the local structure of the polymer. From eq (21), it follows

$$
h_{p,ij}(\boldsymbol{q}) = \frac{12\delta_{ij}f_{pi}}{b^2}\frac{1}{\boldsymbol{q}^2} + \cdots, \qquad \boldsymbol{q}^2 \to \infty
\tag{28}
$$

5

Thus $g_{p,ij}$ is given by

$$g_{p,ij}(\boldsymbol{q}) = \frac{\delta_{ij}b^2}{12f_{pi}}\boldsymbol{q}^2 + \cdots, \qquad \boldsymbol{q}^2 \to \infty \tag{29}$$

The behavior of $g_{p,ij}(\boldsymbol{q})$ for small $\boldsymbol{q}$ region is less obvious. In the limit of $\boldsymbol{q}^2 \to 0$, eq (21) can be expanded into the power series of $\boldsymbol{q}^2$.

$$h_{p,ij}(\boldsymbol{q}) = N_p f_{pi} f_{pj} - H_{p,ij}\boldsymbol{q}^2 + \cdots, \qquad \boldsymbol{q}^2 \to 0 \tag{30}$$

where the expansion coefficient $H_{p,ij}$ is given by

$$H_{p,ij} = \begin{cases} \dfrac{1}{18}N_p^2 f_{pi}^3 b^2 & (i = j) \\ N_p f_{pi} f_{pj} \left[\dfrac{1}{12}N_p(f_{pi} + f_{pj})b^2 + \dfrac{1}{6}l_{p,ij}^2 \right] & (i \neq j) \end{cases} \tag{31}$$

Eq (30) indicates that $\det(h_{p,ij}(\boldsymbol{q}))$ becomes zero at $\boldsymbol{q}^2 = 0$ (since $\det(N_p f_{pi} f_{pj}) = 0$). Therefore the matrix equation (25) becomes singular for $\boldsymbol{q}^2 \to 0$. It is shown in the Appendix A that the solution of eq (25) for small $\boldsymbol{q}$ can be written as

$$g_{p,ij}(\boldsymbol{q}) = \frac{A_{p,ij}}{\boldsymbol{q}^2} + \cdots \qquad \boldsymbol{q}^2 \to 0 \tag{32}$$

where

$$A_{p,ij} = -\left(H_p^{-1}\right)_{ij} + \frac{\sum_{kl} \left(H_p^{-1}\right)_{ik} f_{pk} f_{pl} \left(H_p^{-1}\right)_{lj}}{\sum_{kl} f_{pk} \left(H_p^{-1}\right)_{kl} f_{pl}} \tag{33}$$

where $\left(H_p^{-1}\right)_{ij}$ is the ij component of the inverse matrix of $(H_p)_{ij}$:

$$\sum_k H_{p,ij} \left(H_p^{-1}\right)_{jk} = \delta_{ik} \tag{34}$$

2.3   Approximate Expression for the Vertex Function

Having seen the asymptotic behavior of $g_{p,ij}(\boldsymbol{q})$, we now seek an approximate expression for $g_{p,ij}(\boldsymbol{q})$ which can be used in the entire region of $\boldsymbol{q}$. Considering the asymptotic behavior in the two limits of $\boldsymbol{q}^2 \to 0$ and $\boldsymbol{q}^2 \to \infty$, we use the following expression

$$g_{p,ij}(\boldsymbol{q}) = \frac{A_{p,ij}}{\boldsymbol{q}^2} + C_{p,ij} + \frac{\delta_{ij}b^2}{12f_{pi}}\boldsymbol{q}^2 \tag{35}$$

where the constant $C_{p,ij}$ is chosen so that eq (35) gives a good approximation in the intermediate region. We use the following procedure to determine $C_{p,ij}$.

For $i = j$, $g_{p,ij}(\boldsymbol{q})$ has a minimum at $\boldsymbol{q}^{*2}_{pi} = \sqrt{12 f_{pi} A_{p,ii}/b^2}$. We thus determined $C_{p,ii}$ so that the minimum value agrees with the exact value. This gives

$$C_{p,ii} = \left(h_p^{-1}(\boldsymbol{q}^*_{pi})\right)_{ii} - \frac{A_{p,ii}}{\boldsymbol{q}^{*2}_{pi}} - \frac{b^2}{12f_{pi}}\boldsymbol{q}^{*2}_{pi} \tag{36}$$

where $\left(h_p^{-1}(\boldsymbol{q}^*_{pi})\right)_{ij}$ stands for the ij component of the inverse matrix $h_{p,ij}(\boldsymbol{q})$ at $\boldsymbol{q} = \boldsymbol{q}^*_{pi}$.

For $i \neq j$, $g_{p,ij}(\boldsymbol{q})$ is a monotonically decreasing function of $\boldsymbol{q}^2$ and approaches to a constant value $C_{p,ij}$ for $\boldsymbol{q}^2 \to \infty$. We thus determined $C_{p,ij}$ by $(h_p^{-1}(\infty))_{ij}$. This value is given by (see Appendix A)

$$C_{p,ij} = \begin{cases} -\dfrac{1}{4N_p f_{pi} f_{pj}} & (l_{p,ij}^2 = 0) \\ 0 & (l_{p,ij}^2 \neq 0) \end{cases} \tag{37}$$

6

From eqs (27) and (35), the second order vertex function is obtained as

$$\Gamma_{pi,qj}(\boldsymbol{q}) \approx \frac{\delta_{pq}}{\bar{\phi}_p}\left[\frac{A_{p,ij}}{\boldsymbol{q}^2} + C_{p,ij} + \frac{\delta_{ij}b^2}{12f_{pi}}\boldsymbol{q}^2\right] + \chi_{pi,qj} \tag{38}$$

This gives the following free energy in the real space representation:

$$\begin{aligned}
F\left[\{\phi_{pi}(\boldsymbol{r})\}\right] = {} & F\left[\{f_{pi}\bar{\phi}_p\}\right] \\
& + \sum_{p,ij}\int d\boldsymbol{r}d\boldsymbol{r}' \frac{A_{p,ij}}{2\bar{\phi}_p}\mathcal{G}(\boldsymbol{r}-\boldsymbol{r}')\delta\phi_{pi}(\boldsymbol{r})\delta\phi_{pj}(\boldsymbol{r}') \\
& + \sum_{p,ij}\int d\boldsymbol{r}\,\frac{C_{p,ij}}{2\bar{\phi}_p}\delta\phi_{pi}(\boldsymbol{r})\delta\phi_{pj}(\boldsymbol{r}) \\
& + \sum_{p,i}\int d\boldsymbol{r}\,\frac{b^2}{24f_{pi}\bar{\phi}_p}\left|\nabla\delta\phi_{pi}(\boldsymbol{r})\right|^2 \\
& + \sum_{pi,qj}\int d\boldsymbol{r}\,\frac{\chi_{pi,qj}}{2}\delta\phi_{pi}(\boldsymbol{r})\delta\phi_{qj}(\boldsymbol{r}) \\
& + \cdots
\end{aligned} \tag{39}$$

This free energy functional is valid for $|\delta\phi_{pi}(\boldsymbol{r})| \ll 1$.

2.4 Test of the Approximate Free Energy for Small Perturbation

We now test the accuracy of eq (39) by calculating the density correlation function of block copolymers. The density correlation function $S_{pi,qj}(\boldsymbol{q})$ can be calculated from $\Gamma_{pi,qj}(\boldsymbol{q})$ by solving eq (18). For polymer melts, an additional constraint called the incompressible condition, is usually imposed. This condition is written as

$$\sum_{p,i}\phi_{pi}(\boldsymbol{r}) = 1, \quad \text{or,} \quad \sum_{p,i}\phi_{pi}(\boldsymbol{q}) = 0 \qquad \text{for} \quad \boldsymbol{q} \neq 0 \tag{40}$$

This condition is equivalent to assume the following interaction energy

$$\tilde{\chi}\sum_{pi,qj}\phi_{pi}(\boldsymbol{q})\phi_{qj}(-\boldsymbol{q}) \tag{41}$$

and taking the limit of $\tilde{\chi} \to \infty$. This gives the following density correlation function:

$$S_{pi,qj}(\boldsymbol{q}) = \left(\Gamma^{-1}\right)_{pi,qj}(\boldsymbol{q}) - \frac{\left[\sum_{r,k}\left(\Gamma^{-1}\right)_{pi,rk}(\boldsymbol{q})\right]\left[\sum_{r,k}\left(\Gamma^{-1}\right)_{qj,rk}(\boldsymbol{q})\right]}{\sum_{r,s,k,l}(\Gamma^{-1})_{rk,sl}(\boldsymbol{q})} \tag{42}$$

The second term comes from the incompressible condition.

Figure 2 shows the scattering functions for AB diblock polymer melts for $\chi_{AB} = 0$. Here $S(\boldsymbol{q})$ is defined by

$$S(\boldsymbol{q}) = S_{AA}(\boldsymbol{q}) + S_{BB}(\boldsymbol{q}) - 2S_{AB}(\boldsymbol{q}) \tag{43}$$

The dashed line denote the exact scattering function calculated by eqs (18), (27) and (43). The solid line denote the result of the approximate scattering function calculated by eqs (18), (38) and (43). It is seen that the agreement is quite good.

Figure 3 shows the scattering functions for symmetric ABA triblock polymer melts. The agreement is again quite good.

7

3 General Free Energy Functional

3.1 Free Energy Variation for Phase Separated State

Eq (39) can be used only for the homogeneous state where $|\delta\phi_{pi}(\boldsymbol{r})| \ll 1$. We now seek a general expression for the free energy which can be used for the phase separated state. The expression has to reduce to eq (39) for the case of small deviation from the homogeneous state. Clearly such generalized expression is not unique. The correct way to handle such systems is to evaluate the correlations under inhomogeneous density profile, but it is quite difficult to evaluate them analytically (in most cases, it must be done numerically). In the following, we propose a plausible form of the generalized expression based on physical argument instead, and test its validity for some typical cases.

First we note that, for phase separated state, eq (39) is not valid even if the density deviation $\delta\phi_{pi}(\boldsymbol{r})$ from the equilibrium state is small: for macroscopically phase separated system, $\bar{\phi}_p$ in eq (39) should not be the average of $\phi_p(\boldsymbol{r})$ for the entire volume; it should be the average of $\phi_p(\boldsymbol{r})$ in the local region of the phase separated state where the point $\boldsymbol{r}$ and $\boldsymbol{r}'$ are located. This consideration suggests the following replacement

$$\bar{\phi}_p \to [\phi_p(\boldsymbol{r})\phi_p(\boldsymbol{r}')]^{1/2} \tag{44}$$

However such replacement does not give an analytically tractable form for the free energy. As an alternative, we used the following replacement:

$$\bar{\phi}_p \to \left[\frac{\phi_{pi}(\boldsymbol{r})\phi_{pj}(\boldsymbol{r}')}{f_{pi}f_{pj}}\right]^{1/2} \tag{45}$$

This gives the following free energy functional for small variation of $\phi_{pi}(\boldsymbol{r})$.

$$
\begin{aligned}
\delta^{(2)}F\left[\{\phi_{pi}(\boldsymbol{r})\}\right] =& \\
&\sum_{p,ij}\int d\boldsymbol{r}d\boldsymbol{r}'\,\frac{1}{2}\sqrt{f_{pi}f_{pj}}A_{p,ij}\mathcal{G}(\boldsymbol{r}-\boldsymbol{r}')\frac{\delta\phi_{pi}(\boldsymbol{r})}{\sqrt{\phi_{pi}(\boldsymbol{r})}}\frac{\delta\phi_{pj}(\boldsymbol{r}')}{\sqrt{\phi_{pj}(\boldsymbol{r}')}} \\
&+\sum_{p,ij}\int d\boldsymbol{r}\,\frac{1}{2}\sqrt{f_{pi}f_{pj}}C_{p,ij}\frac{\delta\phi_{pi}(\boldsymbol{r})}{\sqrt{\phi_{pi}(\boldsymbol{r})}}\frac{\delta\phi_{pj}(\boldsymbol{r})}{\sqrt{\phi_{pj}(\boldsymbol{r})}} \\
&+\sum_{pi}\int d\boldsymbol{r}\,\frac{b^2}{24}\frac{|\nabla\delta\phi_{pi}(\boldsymbol{r})|^2}{\phi_{pi}(\boldsymbol{r})} \\
&+\sum_{pi,qj}\int d\boldsymbol{r}\,\frac{\chi_{pi,qj}}{2}\delta\phi_{pi}(\boldsymbol{r})\delta\phi_{qj}(\boldsymbol{r}) \\
&+\cdots
\end{aligned}
\tag{46}
$$

3.2 Free Energy for the General Case

The right hand side of eq.(46) represents the second order functional variation of the functional $F\left[\{\phi_{pi}(\boldsymbol{r})\}\right]$ with respect to $\phi_{pi}(\boldsymbol{r})$. The equation is then regarded as a second order functional differential equation. From the equation, the functional $F\left[\{\phi_{pi}(\boldsymbol{r})\}\right]$ is uniquely determined. The

result is

$$
\begin{aligned}
F\left[\{\phi_{pi}(\boldsymbol{r})\}\right] = \\
&\sum_{p,ij} \int d\boldsymbol{r} d\boldsymbol{r}' \, 2\sqrt{f_{pi}f_{pj}} A_{p,ij} \mathcal{G}(\boldsymbol{r}-\boldsymbol{r}')\sqrt{\phi_{pi}(\boldsymbol{r})\phi_{pj}(\boldsymbol{r}')} \\
&+ \sum_{pi} \int d\boldsymbol{r} \, f_{pi} C_{p,ii}\phi_{pi}(\boldsymbol{r}) \ln \phi_{pi}(\boldsymbol{r}) \\
&+ \sum_{p,i\neq j} \int d\boldsymbol{r} \, 2\sqrt{f_{pi}f_{pj}} C_{p,ij}\sqrt{\phi_{pi}(\boldsymbol{r})\phi_{pj}(\boldsymbol{r})} \\
&+ \sum_{pi} \int d\boldsymbol{r} \, \frac{b^2}{24\phi_{pi}(\boldsymbol{r})} |\nabla \phi_{pi}(\boldsymbol{r})|^2 \\
&+ \sum_{pi,qj} \int d\boldsymbol{r} \, \frac{\chi_{pi,qj}}{2}\phi_{pi}(\boldsymbol{r})\phi_{qj}(\boldsymbol{r})
\end{aligned}
\tag{47}
$$

It is straightforward to check that the second order functional variation of eq (46) with respect to $\delta\phi_{pi}(\boldsymbol{r})$ leads eq (39). This free energy functional does not depend on $\bar{\phi}_p$ and can be used for strong segregation.

Of course there ane many other possible free energy functional which reduces to eq (39), but eq (47) has several advantages.

1. For homopolymer blends, eq (47) gives the Flory-Huggins-de Gennes type [22, 21] (or Lifshitz type [23]) free energy. This is shown in section 4.1.

2. For the ordered phase of diblock copolymers, eq (47) gives the results equivalent to that of the Ohta-Kawasaki theory [13, 14]. This will be demonstrated in section 4.2.

3. The minimization of eq (47) with respect to $\phi_{pi}(\boldsymbol{r})$ usually requires numerical calculation for which eq (47) has an advantage. We found that by using the variable $\psi_{pi}(\boldsymbol{r}) \equiv \sqrt{\phi_{pi}(\boldsymbol{r})}$ rather than $\phi_{pi}(\boldsymbol{r})$ itself, we can improve the numerical stability significantly. The detail of the numerical procedure is described in Appendix B.

4 Test of the Free Energy

In this section we apply the free energy expression (76) to special cases, and discuss its accuracy.

4.1 Homopolymer Blends

For homopolymer, A_p becomes identically equal to zero since eq (33) gives

$$
A_p = -N_p^{-1} + \frac{N_p^{-1}N_p^{-1}}{N_p^{-1}} = 0
\tag{48}
$$

and there is no long range interaction.

C_p can be calculated as follows.

$$
C_p = (h_p(0))^{-1} = \frac{1}{N_p}
\tag{49}
$$

From eq (47), the free energy functional for the system can be described as

$$F\left[\{\phi_p(\boldsymbol{r})\}\right] =$$

$$\sum_p \int d\boldsymbol{r}\, \frac{1}{N_p}\phi_p(\boldsymbol{r})\ln\phi_p(\boldsymbol{r})$$

$$+ \sum_p \int d\boldsymbol{r}\, \frac{b^2}{24\phi_p(\boldsymbol{r})}\left|\nabla\phi_p(\boldsymbol{r})\right|^2 \tag{50}$$

$$+ \sum_{p,q} \int d\boldsymbol{r}\, \frac{\chi_{pq}}{2}\phi_p(\boldsymbol{r})\phi_q(\boldsymbol{r})$$

Thus our free energy functional reduces to the Flory-Huggins-de Gennes type free energy functional [21] (strictly speaking, the free energy given in ref [21] has the factor $1/36$ in the second term of eq (50). This is because in ref [21], the factor is determined from the behavior of $h(\boldsymbol{q})$ for small $\boldsymbol{q}$ region, while we determined it using the behavior for large $\boldsymbol{q}$ region. The factor $1/24$ agree with that given by Lifshitz et. al. [23]).

4.2 Diblock Copolymer Melts

For diblock copolymer melts, A_{ij} and C_{ij} are given by

$$A_{ij} = \frac{9}{N^2 b^2 f^2 (1-f)^2}\begin{bmatrix} (1-f)^2 & -f(1-f) \\ -f(1-f) & f^2 \end{bmatrix} \tag{51}$$

$$C_{ij} = \frac{1}{Nf(1-f)}\begin{bmatrix} s(f) & -1/4 \\ -1/4 & s(1-f) \end{bmatrix} \tag{52}$$

where $b_A = b_B = b, f_A = 1 - f_B = f$ and $s(f)$ is the function which is determined from eqs (36), (37).

From eq (39) the free energy functional for the weak segregation limit will be

$$F\left[\phi(\boldsymbol{r})\right] =$$

$$\int d\boldsymbol{r}d\boldsymbol{r}'\, \frac{9}{2N^2 b^2 f^2 (1-f)^2}\mathcal{G}(\boldsymbol{r}-\boldsymbol{r}')\delta\phi(\boldsymbol{r})\delta\phi(\boldsymbol{r}')$$

$$- \int d\boldsymbol{r}\, \bar{\chi}\delta\phi^2(\boldsymbol{r}) \tag{53}$$

$$+ \int d\boldsymbol{r}\, \frac{b^2}{24f(1-f)}\left|\nabla\delta\phi(\boldsymbol{r})\right|^2$$

$$+ \mathcal{W}\left[\delta\phi(\boldsymbol{r})\right]$$

where we set $\phi(\boldsymbol{r}) = \phi_A(\boldsymbol{r}) = 1 - \phi_B(\boldsymbol{r})$, $F\left[\bar{\phi}\right] = 0$ and $\bar{\chi} = \chi_{AB} - [s(f)+s(1-f)+1/2]/2Nf(1-f)$. $\mathcal{W}\left[\delta\phi(\boldsymbol{r})\right]$ is the contribution of the higher order terms for $\delta\phi(\boldsymbol{r})$. In this case the free energy functional reduces to the Ohta-Kawasaki type free energy functional [13].

For strong segregation, we get the following free energy functional from eq (47).

$$F\left[\phi(\boldsymbol{r})\right] =$$

$$\int d\boldsymbol{r}d\boldsymbol{r}'\, \frac{18}{N^2 b^2 f(1-f)}\mathcal{G}(\boldsymbol{r}-\boldsymbol{r}')\tau(\boldsymbol{r})\tau(\boldsymbol{r}')$$

$$+ \int d\boldsymbol{r}\, \frac{1}{N}\left[\frac{s(f)}{1-f}\phi(\boldsymbol{r})\ln\phi(\boldsymbol{r}) + \frac{s(1-f)}{f}\left(1-\phi(\boldsymbol{r})\right)\ln\left(1-\phi(\boldsymbol{r})\right)\right]$$

$$- \int d\boldsymbol{r}\, \frac{1}{N\sqrt{f(1-f)}}\sqrt{\phi(\boldsymbol{r})\left(1-\phi(\boldsymbol{r})\right)} \tag{54}$$

$$+ \int d\boldsymbol{r}\, \frac{b^2}{24\phi(\boldsymbol{r})\left(1-\phi(\boldsymbol{r})\right)}\left|\nabla\phi(\boldsymbol{r})\right|^2$$

$$+ \int d\boldsymbol{r}\, \chi\phi(\boldsymbol{r})\left(1-\phi(\boldsymbol{r})\right)$$

10

where $\tau(\boldsymbol{r}) \equiv \sqrt{(1-f)\phi(\boldsymbol{r})} - \sqrt{f(1-\phi(\boldsymbol{r}))}$ and $\chi = \chi_{AB}$. The interfacial energy in eq (54) (the fourth term) does not depend on f. This is consistent with the improved form of the Ohta-Kawasaki theory [14].

Figure 4 shows the phase diagram for AB diblock copolymer melts. The solid line is the results of the DF theory and the dashed line is the result of Matsen Bates [11] which is based on the SCF theory. The critical point predicted by our DF is $\chi N = 10.553778$, while that predicted by the SCF theory is $\chi N = 10.495$. The results of the DF and the SCF do not agree quantitatively but they agree well qualitatively. Especially notice that the DF gives a stable double gyroid phase between the lamellar and the hexagonal cylinder phase for small χN. It is difficult to get such a result by the previous density functional theories (the Leibler theory or the Ohta-Kawasaki theory).

Figures 5 shows the equilibrium periods for AB diblock copolymer melts plotted against χN. Our DF theory does not agree well with the SCF theory, but it reproduces the scaling feature correctly: $D \propto N^{1/2}$ for weak segregation and $D \propto N^{3/2}$ for strong segregation. The numerical disagreement is the nature of the Ohta-Kawasaki type approximation and arises from the approximation for the vertex functions (eq (38)).

Figures 6 shows the equilibrium density profile of AB diblock copolymer melts. The solid line is the results of the DF theory and the dashed line is the result of the SCF theory[11]. The result of the DF theory deviates significantly from that of SCF theory for weak segregation, while they become close to each other for strong segregation.

4.3   A,B Homopolymer / AB Diblock Copolymer Blends

We applied eq (76) to A,B homopolymer / AB diblock copolymer blends. The free energy model for A,B homopolymer / AB diblock copolymer melts was proposed and studied by Kawakatsu [18]. Our free energy functional has similar form to the Kawakatsu's theory.

Figure 7 is equilibrium structures for an A,B homopolymer / AB diblock copolymer blend. We set $\bar{\phi}_A = \bar{\phi}_B = 0.475, \bar{\phi}_{AB} = 0.05, N_A = N_B = N_{AB} = 40, f_{AB,A} = f_{AB,B} = 0.5, \chi_{AB} = 1$. The result of the SCF theory was obtained by using the SUSHI engine in OCTA system [25]. Again the agreement between the DF theory and the SCF theory is not perfect, but reasonable considering that no adjustable parameter is used in these comparison.

4.4   AB diblock coplymer / C homopolymer blends

As the last example, we show the results of AB diblock copolymer / C homopolymer blends [17]. These blends cause the macrophase separation as well as the microphase separation and show various interesting structures. Figures 8 and 9 are equilibrium structures for AB diblock copolymer / C homopolymer blends (the parameters are $N_{AB} = 10, N_C = 20, f_{AB,A} = f_{AB,B} = 0.5, \bar{\phi}_{AB} = 0.2, \bar{\phi}_C = 0.8, \chi_{AB} = 1.2, \chi_{BC} = 1, \chi_{CA} = 0.5$ and $N_{AB} = 10, N_C = 20, f_{AB,A} = 0.35, f_{AB,B} = 0.65, \bar{\phi}_{AB} = 0.3, \bar{\phi}_C = 0.7, \chi_{AB} = 1.75, \chi_{BC} = 1, \chi_{CA} = 0.5$, respectively). The simulation has been done for the three dimensional periodic system of $64 \times 64 \times 64$ lattice points (the system size is $40b \times 40b \times 40b$). The structure of the AB diblock copolymer in Figure 8 is considered to be the "onion structure" observed by the experiments [26]. It is also noted that each simulation starts from the homogeneous state, and gives the results shown there after about 4 hours on the 3.0GHz Xeon workstation. It is quite difficult to get these results with such short computational time by the SCF simulation.

4.5   Comparison with the other density functional theory

In this section, we compare our theory with the density functional theory proposed by Bohbot-Raviv and Wang for block copolymer melts [19]. They used the Flory-Huggins free energy for the disconnected blocks as the reference and took into account of the effect of chain correlation by the

second order vertex function with the RPA: their free energy functional is expressed as

$$F\left[\{\phi_i(\boldsymbol{r})\}\right] = F_{\text{ref}}\left[\{\phi_i(\boldsymbol{r})\}\right] + \Delta F\left[\{\Delta\phi_i(\boldsymbol{q})\}\right] \tag{55}$$

$$F_{\text{ref}}\left[\{\phi_i(\boldsymbol{r})\}\right] = \sum_i \int d\boldsymbol{r}\, \frac{1}{f_i N}\phi_i(\boldsymbol{r})\ln\phi_i(\boldsymbol{r}) \tag{56}$$

$$\begin{aligned}
\Delta F\left[\{\Delta\phi_i(\boldsymbol{q})\}\right] =& \frac{1}{2}\sum_{i,j}\frac{1}{(2\pi)^d}\int d\boldsymbol{q}\,\Gamma_{i,j}(\boldsymbol{q})\Delta\phi_i(\boldsymbol{q})\Delta\phi_j(-\boldsymbol{q}) \\
&- \frac{1}{2}\sum_i \frac{1}{(2\pi)^d}\int d\boldsymbol{q}\frac{1}{f_i N}\Delta\phi_i(\boldsymbol{q})\Delta\phi_i(-\boldsymbol{q})
\end{aligned} \tag{57}$$

where

$$\Delta\phi_i(\boldsymbol{r}) = \phi_i(\boldsymbol{r}) - f_i \tag{58}$$

Eq (55) is exactly same as eq (2) except for higher order terms for $\Delta\phi_i(\boldsymbol{r})$ (it can be easily shown by setting $\bar{\phi} = 1$ and expanding eq (55) by series of $\Delta\phi_i(\boldsymbol{r})$).

Though their approach is simple and straightforward their theory cannot overcome one well-known difficulty. Ohta and Kawasaki noticed that the block ratio dependence of the interfacial tension calculated from the RPA is inconsistent with other theories [14]. They then proposed to replace f, the block ratio, by the local density $\phi(\boldsymbol{r})$. Without this correction, the free energy eq (55) cannot give correct block ratio dependence. The replacement eq (45) is essentially same as the replacement by Ohta and Kawasaki and therefore our free energy (76) does not have such difficulty.

5 Conclusion

We have given an expression of the free energy of blends of block copolymers expressed as a functional of the density distribution of monomers in each block. All parameters in the expression are determined by the polymer structure parameter (such as the degree of polymerization, the branching structure, and block ratio etc.) and the χ parameter. For homopolymer blends, the expression is shown to reduce to the Flory-Huggins-de Gennes theory. For diblock copolymer melts, the expression gives results equivalent to the Ohta-Kawasaki theory. Thus the expression is expected to work in more general case. We have applied the expression for several cases, and found reasonable agreement with the SCF calculation. Of course, these examples do not guarantee the validity of our approximation in the general case, and more work is clearly needed to test the validity of our expression.

The present theory is most useful by combining it to the SCF calculation. It uses exactly the same parameter set as the SCF theory (this is in contrast to the other mesoscopic approaches such as the dissipative particle dynamics (DPD) [27]). Therefore the theory can be used to get the initial structure for the SCF calculation, or it can be used to get an overview of the phase diagram of block copolymers. These applications will be pursued in future.

Acknowledgment

Appendix

A   Calculation of $A_{p,ij}$ and $C_{p,ij}$

A.1   Calculation of $A_{p,ij}$

In this section we derive eq (33). At the limit of $\boldsymbol{q}^2 \to 0$, $h_{p,ij}(\boldsymbol{q})$ can be expanded as follows.

$$h_{p,ij}(\boldsymbol{q}) = N_p f_{pi} f_{pj} - H_{p,ij} \boldsymbol{q}^2 + \cdots \tag{59}$$

where $H_{p,ij}$ is given by eq (31). As we are considering one ideal chain, we omit the subscript "p" and describe eq (59) in a matrix form.

$$\boldsymbol{h}(\boldsymbol{q}) = N \boldsymbol{f} \boldsymbol{f}^t - \boldsymbol{H} \boldsymbol{q}^2 + \cdots \tag{60}$$

where $\boldsymbol{f}^t$ is the transposed vector of $\boldsymbol{f}$.

We obtain $\boldsymbol{g}(\boldsymbol{q})$, the inverse matrix of $\boldsymbol{h}(\boldsymbol{q})$, in the following form:

$$\boldsymbol{g}(\boldsymbol{q}) = \boldsymbol{A} \frac{1}{\boldsymbol{q}^2} + \boldsymbol{B} + \cdots \tag{61}$$

From eq (25),

$$\boldsymbol{g}(\boldsymbol{q}) \cdot \boldsymbol{h}(\boldsymbol{q}) = \left(\boldsymbol{A} \frac{1}{\boldsymbol{q}^2} + \boldsymbol{B} + \cdots \right) \cdot \left(N \boldsymbol{f} \boldsymbol{f}^t - \boldsymbol{H} \boldsymbol{q}^2 + \cdots \right) = \boldsymbol{E} \tag{62}$$

and we get the following set of equations.

$$\boldsymbol{A} \cdot \boldsymbol{f} = 0 \tag{63}$$
$$- \boldsymbol{A} \cdot \boldsymbol{H} + N \boldsymbol{B} \cdot \boldsymbol{f} \boldsymbol{f}^t = \boldsymbol{E} \tag{64}$$

where $\boldsymbol{E}$ is unit matrix. Notice that the matrix $\boldsymbol{h}(\boldsymbol{q})$ is symmetric and therefore the matrices $\boldsymbol{A}$ and $\boldsymbol{B}$ are also symmetric. Multiplying $\boldsymbol{H}^{-1} \cdot \boldsymbol{f} \boldsymbol{f}^t$ to eq (64) from the left side and using the relation $\boldsymbol{f}^t \cdot \boldsymbol{A} = (\boldsymbol{A} \cdot \boldsymbol{f})^t = 0$ which follows from eq (63), we get

$$N \boldsymbol{B} \cdot \boldsymbol{f} \boldsymbol{f}^t \cdot \boldsymbol{H}^{-1} \cdot \boldsymbol{f} \boldsymbol{f}^t = \boldsymbol{H}^{-1} \cdot \boldsymbol{f} \boldsymbol{f}^t \tag{65}$$

Since $\boldsymbol{f}^t \cdot \boldsymbol{H}^{-1} \cdot \boldsymbol{f}$ is a scalar, eq (65) gives

$$N \boldsymbol{B} \cdot \boldsymbol{f} \boldsymbol{f}^t = \frac{\boldsymbol{H}^{-1} \cdot \boldsymbol{f} \boldsymbol{f}^t}{\boldsymbol{f}^t \cdot \boldsymbol{H}^{-1} \cdot \boldsymbol{f}} \tag{66}$$

From eqs (64) and (66) we have

$$\boldsymbol{A} = -\boldsymbol{H}^{-1} + \frac{\boldsymbol{H}^{-1} \cdot \boldsymbol{f} \boldsymbol{f}^t \cdot \boldsymbol{H}^{-1}}{\boldsymbol{f}^t \cdot \boldsymbol{H}^{-1} \cdot \boldsymbol{f}} \tag{67}$$

This gives eq (33).

A.2   Calculation of $C_{p,ij}$

In this section we calculate the asymptotic value of $g_{p,ij}(\boldsymbol{q})$ at $\boldsymbol{q}^2 \to \infty$ for $i \neq j$. From eq (21), $h_{p,ij}(\boldsymbol{q})$ can be described as follows in matrix representation.

$$\boldsymbol{h}(\boldsymbol{q}) = \boldsymbol{G} \frac{1}{\boldsymbol{q}^2} + \boldsymbol{K} \frac{1}{\boldsymbol{q}^4} + \cdots \tag{68}$$

where

$$G = \frac{12 f_i \delta_{ij}}{b^2} \tag{69}$$

$$K = \begin{cases} -\dfrac{72}{Nb^4} & (i = j) \\ \dfrac{36}{Nb^4} & (i \neq j, l_{ij}^2 = 0) \\ 0 & (i \neq j, l_{ij}^2 \neq 0) \end{cases} \tag{70}$$

$g_{p,ij}(\boldsymbol{q})$ can be expressed as power series of $\boldsymbol{q}^2$.

$$g(\boldsymbol{q}) = B\boldsymbol{q}^2 + C + \cdots \tag{71}$$

The equations to determine coefficients are

$$BG = E \tag{72}$$
$$BK + CG = 0 \tag{73}$$

Thus we get

$$C = -BKG^{-1} = -G^{-1}KG^{-1}$$
$$= \begin{cases} \dfrac{1}{2f_i^2 N} & (i = j) \\ -\dfrac{1}{4f_i f_j N} & (i \neq j, l_{ij}^2 = 0) \\ 0 & (i \neq j, l_{ij}^2 \neq 0) \end{cases} \tag{74}$$

This gives eq (37).

B Numerical Scheme

The minimization of eq (47) with respect to $\phi_{pi}(\boldsymbol{r})$ usually requires the numerical calculation. Here we briefly describe the numerical scheme we employed.

For numerical calculation, it is convenient to introduce a new order parameter $\psi_{pi}(\boldsymbol{r})$.

$$\psi_{pi}(\boldsymbol{r}) \equiv \sqrt{\phi_{pi}(\boldsymbol{r})} \tag{75}$$

For this order parameter, the free energy functional is written as

$$\begin{aligned}
F\left[\{\psi_{pi}(\boldsymbol{r})\}\right] = \\
&\sum_{p,ij} \int d\boldsymbol{r} d\boldsymbol{r}' \, 2\sqrt{f_{pi} f_{pj}} A_{p,ij} \mathcal{G}(\boldsymbol{r} - \boldsymbol{r}') \psi_{pi}(\boldsymbol{r}) \psi_{pj}(\boldsymbol{r}') \\
&+ \sum_{pi} \int d\boldsymbol{r} \, 2 f_{pi} C_{p,ii} \psi_{pi}^2(\boldsymbol{r}) \ln \psi_{pi}(\boldsymbol{r}) \\
&+ \sum_{p,i \neq j} \int d\boldsymbol{r} \, 2\sqrt{f_{pi} f_{pj}} C_{p,ij} \psi_{pi}(\boldsymbol{r}) \psi_{pj}(\boldsymbol{r}) \\
&+ \sum_{pi} \int d\boldsymbol{r} \, \frac{b^2}{6} |\nabla \psi_{pi}(\boldsymbol{r})|^2 \\
&+ \sum_{pi,qj} \int d\boldsymbol{r} \, \frac{\chi_{pi,qj}}{2} \psi_{pi}^2(\boldsymbol{r}) \psi_{qj}^2(\boldsymbol{r})
\end{aligned} \tag{76}$$

14

This expression is advantageous for numerical calculation as it does not have the numerical instability associated with the logarithmic term of eq (47). The fourth term in eq (76) is in agreement with that proposed by Lifshitz [24, 23].

The equilibrium structure is obtained by minimizing the free energy (76) under the following constraints

$$\sum_{pi} \psi_{pi}^2(\boldsymbol{r}) = 1 \tag{77}$$

$$\int d\boldsymbol{r} \psi_{pi}^2(\boldsymbol{r}) = V f_{pi} \bar{\phi}_p \tag{78}$$

The first equation represents the incompressible condition, and the second equation represents the mass conservation for each block. To take into account of these constraints we use the Lagrangian multiplier method, and added the following terms to eq (76).

$$F_{\text{constraint}}\left[\{\psi_{pi}(\boldsymbol{r})\}\right] = \sum_{pi} \int d\boldsymbol{r} \frac{1}{2}\left[\lambda_{pi} + \kappa(\boldsymbol{r})\right]\left(\psi_{pi}^2(\boldsymbol{r}) - f_{pi}\bar{\phi}_p\right) \tag{79}$$

where λ_{pi} and $\kappa(\boldsymbol{r})$ are the Lagrangian multipliers.

We used simple relaxation method to get equilibrium structures.

$$\psi_{pi}^{(n+1)}(\boldsymbol{r}) = \psi_{pi}^{(n)}(\boldsymbol{r}) - \omega \mu_{pi}^{(n)}(\boldsymbol{r}) \tag{80}$$

where the superscript (n) means the number of the relaxation step, ω is a sufficiently small constant and $\mu_{pi}(\boldsymbol{r})$ is the chemical potential defined as follows.

$$
\begin{aligned}
\mu_{pi}(\boldsymbol{r}) \equiv & \frac{\delta F\left[\{\psi_{pi}(\boldsymbol{r})\}\right]}{\delta \psi_{pi}(\boldsymbol{r})} + \frac{\delta F_{\text{constraint}}\left[\{\psi_{pi}(\boldsymbol{r})\}\right]}{\delta \psi_{pi}(\boldsymbol{r})} \\
= & \sum_{j} 4\sqrt{f_{pi}f_{pj}} A_{p,ij} \int d\boldsymbol{r}' \mathcal{G}(\boldsymbol{r} - \boldsymbol{r}')\psi_{pj}(\boldsymbol{r}') \\
& + 2f_{pi}C_{p,ii}\left[2\psi_{pi}(\boldsymbol{r})\ln\psi_{pi}(\boldsymbol{r}) + \psi_{pi}(\boldsymbol{r})\right] \\
& + \sum_{j(j\neq i)} 4\sqrt{f_{pi}f_{pj}} C_{p,ij}\psi_{pj}(\boldsymbol{r}) \\
& - \frac{b^2}{3}\nabla^2\psi_{pi}(\boldsymbol{r}) \\
& + \sum_{qj} 2\chi_{pi,qj}\psi_{pi}(\boldsymbol{r})\psi_{qj}^2(\boldsymbol{r}) \\
& + \left[\lambda_{pi} + \kappa(\boldsymbol{r})\right]\psi_{pi}(\boldsymbol{r})
\end{aligned}
\tag{81}
$$

The terms including $\mathcal{G}(\boldsymbol{r} - \boldsymbol{r}')$ or ∇^2 are calculated by using the fast Fourier transform (the FFTW library [28] is used), and other terms are calculated in the real space. It is noted that eq (81) has no singularity at $\psi_{pi}(\boldsymbol{r}) = 0$ while $\delta F\left[\{\phi_{pi}(\boldsymbol{r})\}\right]/\delta\phi_{pi}(\boldsymbol{r})$, the chemical potential for $\phi_{pi}(\boldsymbol{r})$, is singular at $\phi_{pi}(\boldsymbol{r}) = 0$. Thus using the order parameter $\psi_{pi}(\boldsymbol{r})$ rather that $\phi_{pi}(\boldsymbol{r})$ improves the numerical stability significantly.

The numerical method we employed in this work is not so efficient We employed this method for simplicity, but the algorithm need to be improved (for example, the ICCG method will improve the convergence).

References

[1] Bates, F. S.; Fredrickson, G. H. *Phys. Today*, **1999**, *52*, 32.

[2] Helfand, E.; Wasserman Z. R. *Macromolecules*, **1976**, *9*, 879. Helfand, E.; Wasserman Z. R. **1978**, *11*, 960. Helfand, E.; Wasserman Z. R. **1980**, *13*, 994.

[3] Matsen, M. W.; Schick M. *Phys. Rev. Lett.*, **1994**, *72*, 2660.

[4] Matsen, M. W. *Macromolecules*, **2003**, *36*, 9647.

[5] Fraaije, J. G. E. M. *J. Chem. Phys.*, **1993**, *99*, 9202.

[6] Zvelindovsky, A. V. M.; van Vlimmeren, B. A. C.; Sevink, G. J. A.; Maurits, N. M.; Fraaije, J. G. E. M. *J. Chem. Phys.*, **1998**, *109*, 8751. Zvelindovsky, A. V. M.; van Vlimmeren, B. A. C.; Sevink, G. J. A.; Maurits, N. M.; Fraaije, J. G. E. M. *Phys. Rev. E*, **1998**, *57*, R4879.

[7] van Vlimmeren, B. A. C.; Maurits, N. M.; Zvelindovsky, A. V. M.; Sevink,G. J. A. ;Fraaije, J. G. E. M. *Macromolecules*, **1999**, *32*, 646.

[8] Drollet, F.; Fredrickson, G. H. *Phys. Rev. Lett.*, **1999**, *83*, 4317.

[9] Ganesan, V.; Fredrickson, G. H. *Europhys. Lett.*, **2001**, *55*, 814; Fredrickson, G. H.; Ganesan, V.; Drollet, F. *Macromolecules*, **2002**, *35*, 16.

[10] Kawakatsu, T. *Statistical Physics of Polymers*; Springer-Verlag: Berlin, 2004.

[11] Matsen, M. W.; Bates, F. S. *Macromolecules*, **1996**, *29*, 1091.

[12] Leibler, L. *Macromolecules*, **1980**, *13*, 1602.

[13] Ohta, T.; Kawasaki, K. *Macromolecules*, **1986**, *19*, 2621.

[14] Ohta, T.; Kawasaki, K. *Macromolecules*, **1990**, *23*, 2413.

[15] Nakazawa, H.; Ohta, T. *Macromolecules*, **1993**, *26*, 5503.

[16] Ren, X.; Wei, J. *Physica D*, **2003**, *178*, 103.

[17] Ohta, T.; Ito, A. *Phys. Rev. E*, **1995**, *52*, 5250.

[18] Kawakatsu, T. *Phys. Rev. E*, **1994**, *50*, 2856.

[19] Bohbot-Raviv, Y.; Wang, Z.-G. *Phys. Rev. Lett.*, **2000**, *85*, 3428

[20] de Gennes, P. G. *Scaling Concepts in Polymer Physics*; Cornell University Press: Ithaca, NY, 1979.

[21] de Gennes, P. G. *J. Chem. Phys.*, **1980**, *72*, 4756.

[22] Joanny, J. F.; Leibler, L. *J. Phys. (Paris)*, **1978**, *39*, 951.

[23] Grosberg, A. Y.; Khokhlov, A. R. *Statistical Physics of Macromolecules*; American Institute of Physics: New York, 1994.

[24] Lifshitz, I. M. *Sov. Phys. JETP*, **1969**, *28*, 1280.

[25] Honda, T. *et. al. SUSHI users manual*, OCTA (http://octa.jp).

[26] Koizumi, S.; Hasegawa, H. ; Hashimoto, T. *Macromolecules*, **1994**, *27*, 6532.

[27] Groot, R. D.; Warren, P. B. *J. Chem. Phys.*, **1997**, *107*, 4423. Groot, R. D.; Madden, T. J. *J. Chem. Phys.*, **1998**, *108*, 8713. Groot, R. D.; Madden, T. J.; Tildesley, D. J. *J. Chem. Phys.*, **1999**, *110*, 9739.

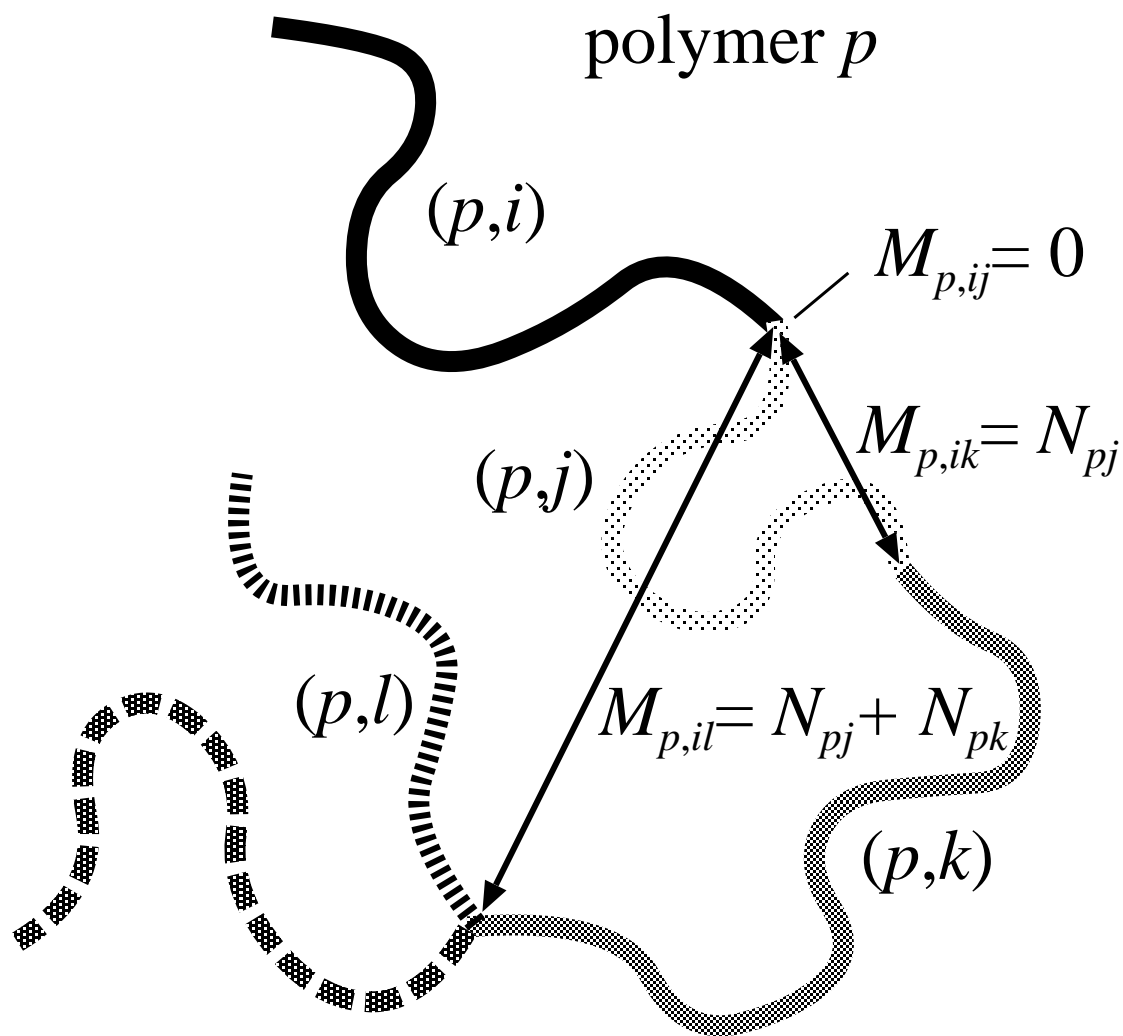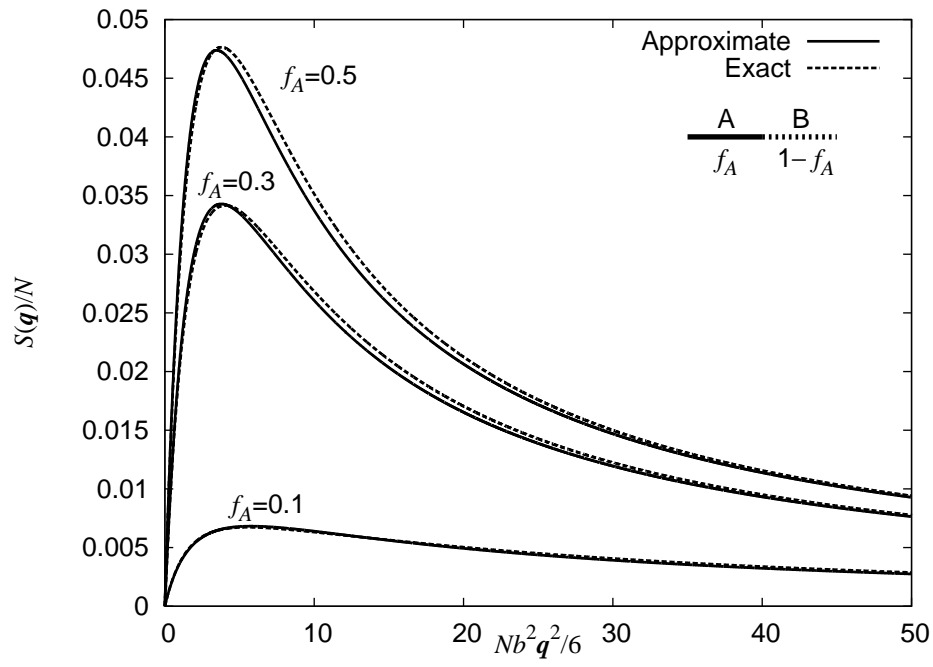[28] Frigo, M.; Johnson, S. G. *Proc. ICASSP*, **1998**, *3*, 1381.

polymer p

(p,i)

$M_{p,ij} = 0$

$M_{p,ik} = N_{pj}$

(p,j)
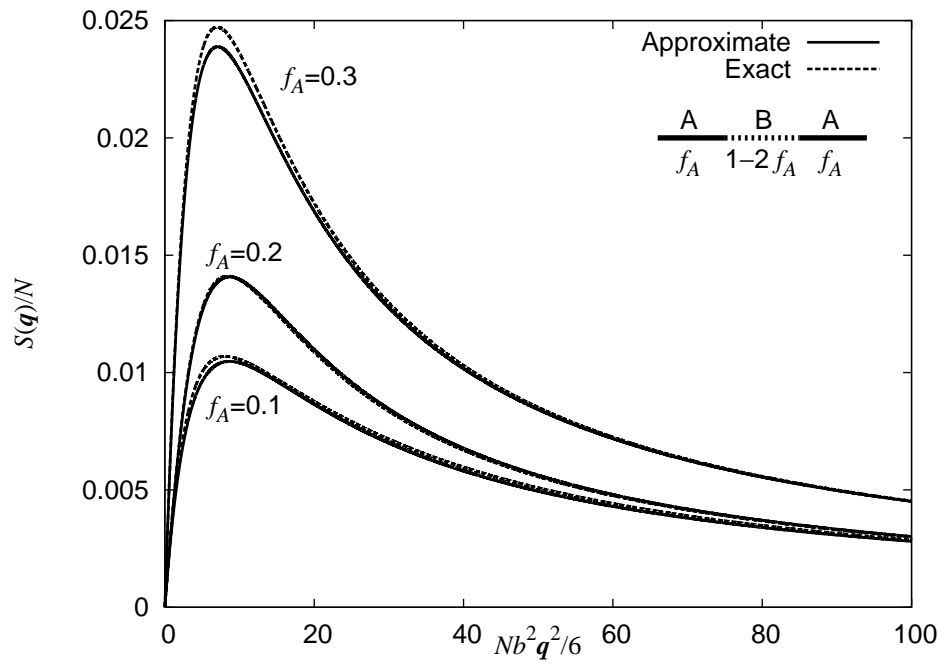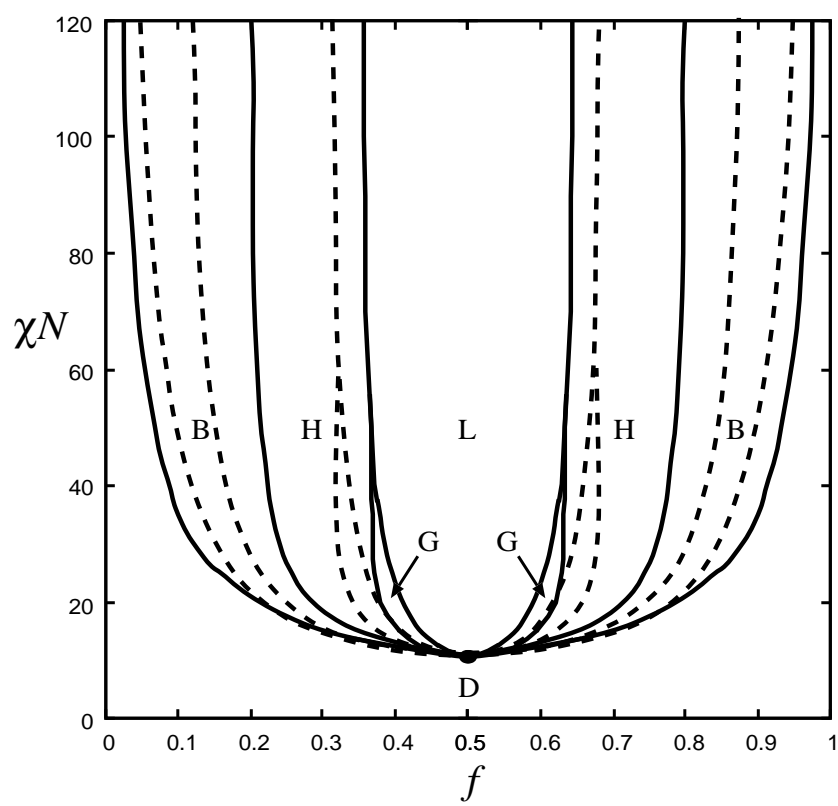
(p,l)

$M_{p,il} = N_{pj} + N_{pk}$
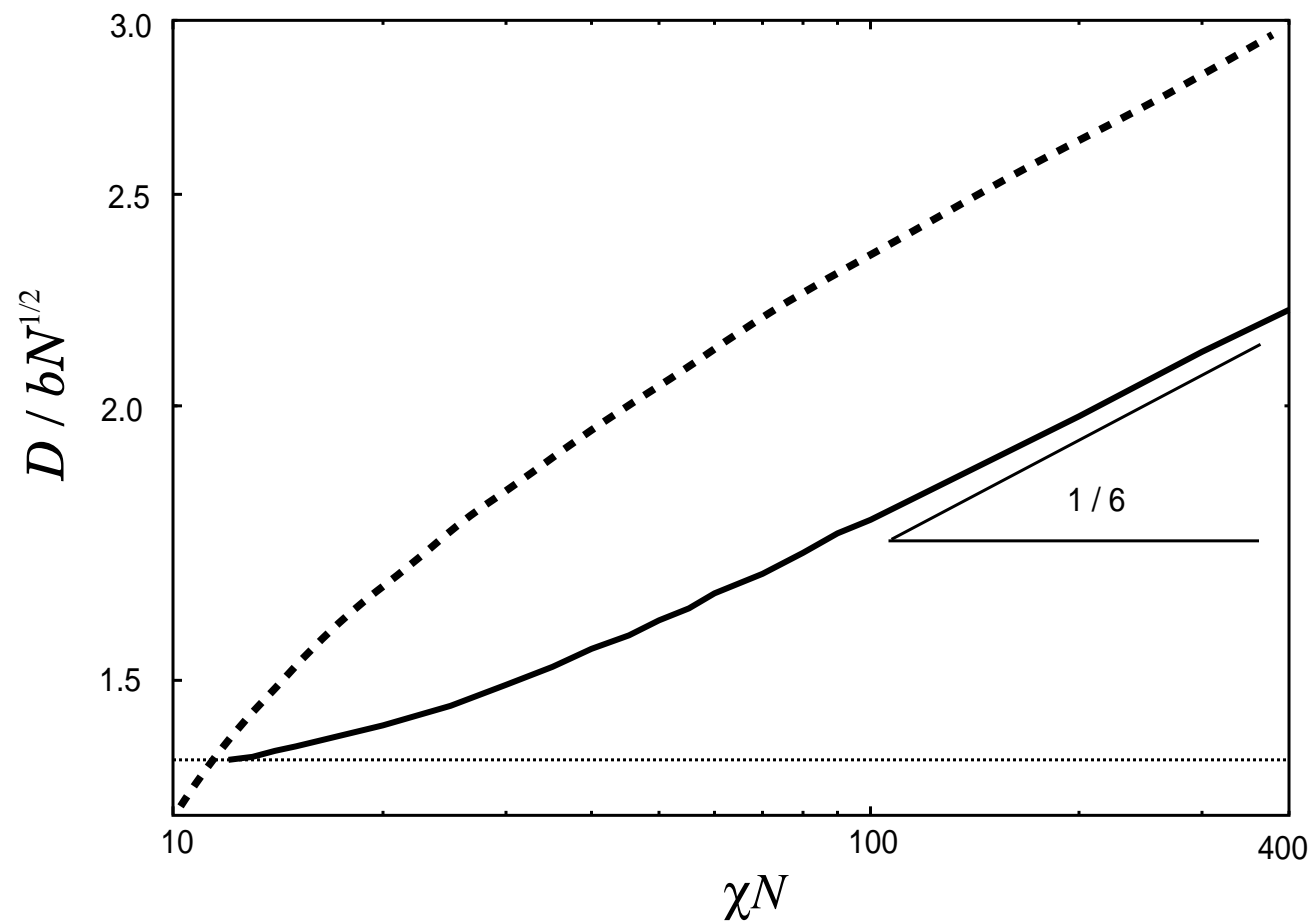
(p,k)

Figure 1:
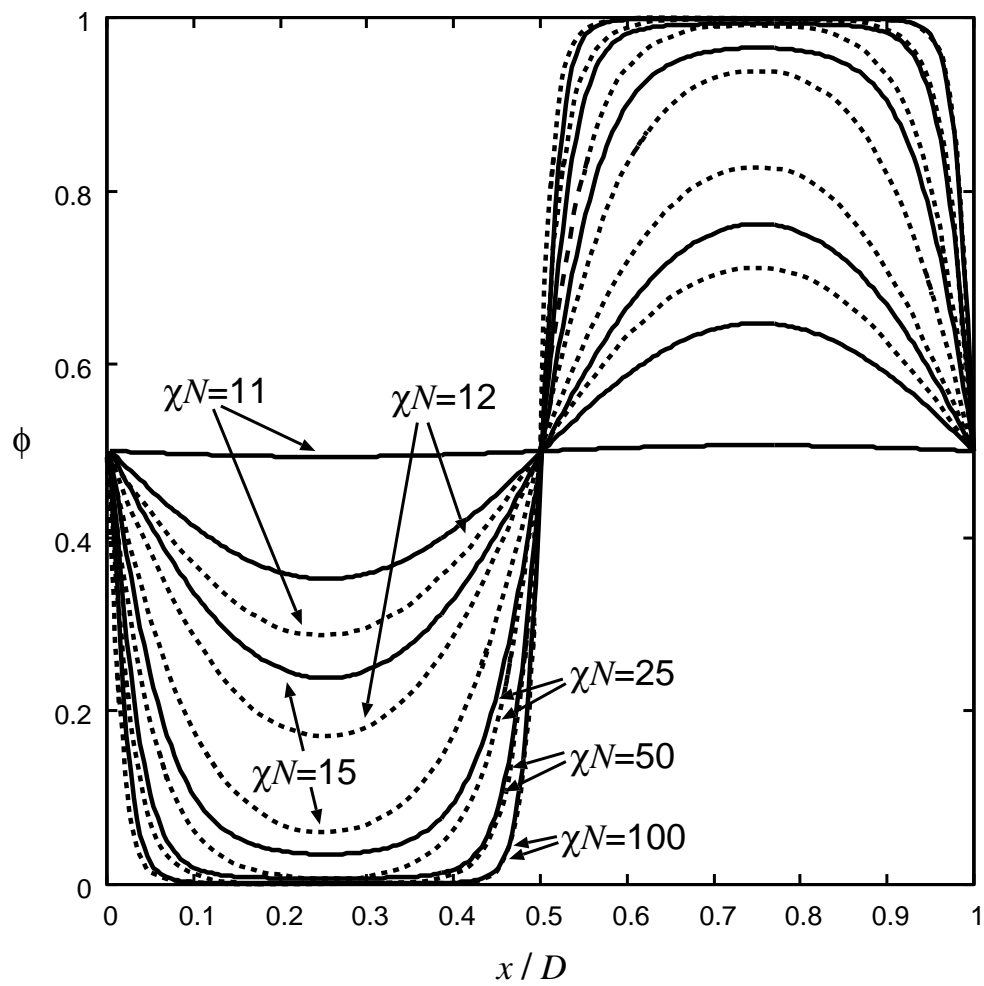
Figure 2:

Figure 3:

18

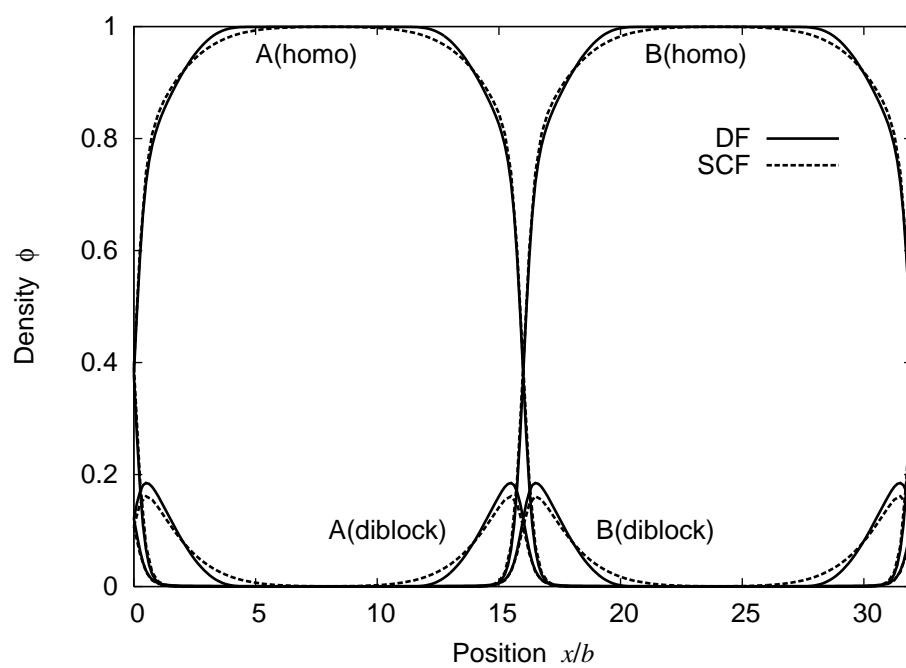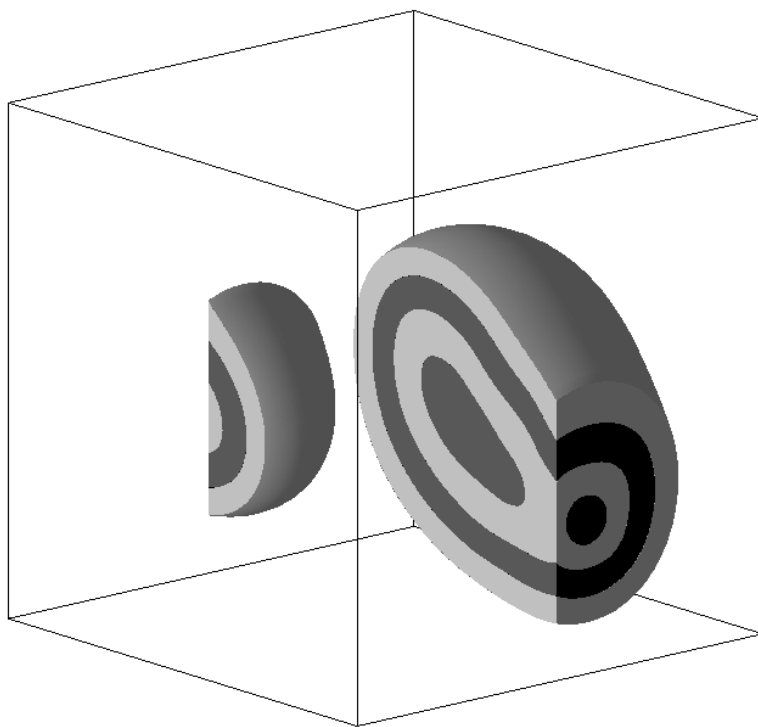Figure 4:

Figure 5:
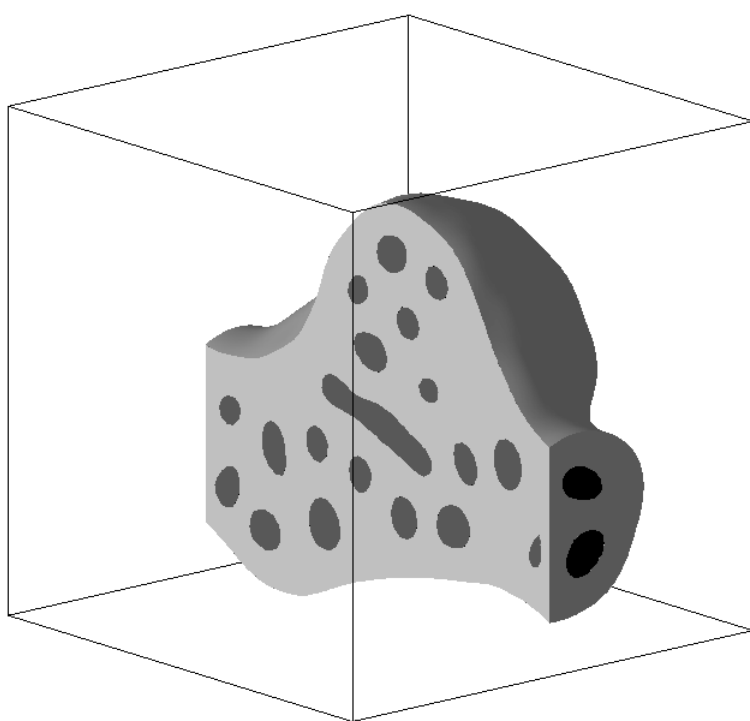
Figure 6:

Figure 7:

Figure 8:

Figure 9:

Figure 1: Chemical distance $M_{p,ij}$ of block copolymers

Figure 2: Scattering functions of AB diblock copolymer melts. The χ parameter χ_{AB} is set to zero, and f_A stands for the block ratio.

Figure 3: Scattering functions of symmetric ABA triblock polymer melts. The χ parameter χ_{AB} is set to zero, and f_A stands for the block ratio defined in the figure.

Figure 4: Phase diagram for AB diblock copolymer melts. The solid lines are the results of the DF simulation and the dashed lines are the results of the SCF simulation [11]. (B: BCC sphere, H: Hexagonal cylinder, G: Double gyroid, L: Lamellar, D: Disordered)

Figure 5: Equilibrium periods for AB diblock copolymer melts. Here D is the equilibrium periods for lamellar structure. The solid lines are the results of the DF simulation and the dashed lines are the results of the SCF simulation [11]. The doted line is calculated by the DF for the weak segregation limit.

Figure 6: Equilibrium structures for AB diblock copolymer melts. The solid line is the result of the DF simulation, the doted line is the analytic solution for weak segregation limit by the DF and the dashed line is the results of the SCF simulation [11].

Figure 7: An equilibrium structures for an A,B homopolymer / AB diblock copolymer blend

Figure 8: An equilibrium structures for an AB diblock coplymer / C homoploymer blend. The black and gray surfaces are the isodensity surface $(\phi_{pi}(\boldsymbol{r}) = 0.5)$ for the A and B segment, respectively.

Figure 9: An equilibrium structures for an AB diblock copolymer / C homopolymer blend. The black and gray surfaces are the isodensity surface $(\phi_{pi}(\boldsymbol{r}) = 0.5)$ for the A and B segment, respectively.